

Electron Quantization in Broken Atomic Wires

Eui Hwan Do and Han Woong Yeom*

*Center for Artificial Low Dimensional Electronic Systems, Institute for Basic Science (IBS),
77 Cheongam-Ro, Pohang 790-784, Korea*

and Department of Physics, Pohang University of Science and Technology (POSTECH), Pohang 790-784, Korea
(Received 1 May 2015; revised manuscript received 17 September 2015; published 28 December 2015)

We demonstrate using scanning tunneling microscopy and spectroscopy the electron quantization within metallic Au atomic wires self-assembled on a Si(111) surface and segmented by adatom impurities. The local electronic states of wire segments with a length up to 10 nm are investigated as terminated by two neighboring Si adatoms. One-dimensional (1D) quantum well states are well resolved by their spatial distributions and the inverse-length-square dependence in their energies. The quantization also results in the quantum oscillation of the conductance at Fermi level. The present approach provides a new and convenient platform to investigate 1D quantum phenomena with atomic precision.

DOI: 10.1103/PhysRevLett.115.266803

PACS numbers: 73.20.At, 68.37.Ef, 68.43.Fg, 73.21.Fg

One-dimensional (1D) materials systems have been investigated extensively because both of the intriguing and exotic nature of their electrons and of interest in nano- or atomic-scale devices. Characteristic 1D electronic properties of fundamental interest include the Tomonaga-Luttinger liquid [1,2], the charge-density wave [3,4], unconventional superconductivity [5], and, more recently, Majorana Fermions [6,7]. However, 1D materials systems are notorious in their intrinsic susceptibility to extrinsic perturbations such as defects and impurities [8–10]. In microscopic points of view, defects or impurities can have various different actions, local or global doping, local lattice distortions, weak or strong electron scatterings, and so on. Nevertheless, the direct atomic-scale investigation on those actions has been far from sufficient.

The self-assembled atomic wire structure of the Si(111)-(5 × 2)-Au surface is an excellent candidate system for a systematic study on interactions of impurities with atomic-scale precision. This system has a well-ordered Au-Si atomic wire array with a well-defined 1D metallic band [11]. Its atomic structure has been debated for a long time but very recently determined conclusively [12,13]. This surface is intrinsically endowed with Si adatom impurities ejected from the Si substrate [14,15], whose density can be controlled globally [11] or in an atom-by-atom fashion [16]. The electronic band structure is systematically tuned by the adatom density from a metal to a gapped insulator globally [11] or locally [17]. This controllability opens up an unprecedented possibility for a systematic study of impurity effects in an atomic-scale 1D metallic system [18].

For quite a long time, a Si adatom on this model 1D system was believed to act as a charged impurity [19], and a recent scanning tunneling microscopy and spectroscopy (STM/S) work claimed the observation of the doping effect of individual adatoms [20]. Within this picture, an impurity atom acts only to locally shift the energy of the 1D metallic

state while the electron scattering and the Friedel oscillation [21] by the impurity are largely neglected. In this Letter, we focus on the electron scattering by a Si adatom. The electron scattering by a single impurity would induce 1D standing waves and that by two neighboring impurities could create the 1D quantum confinement. The latter is fully analogous to the vertical quantization in metallic ultrathin films [22–30], where quantum well states (QWSs) were spectroscopically observed and the density-of-states (DOS) oscillation at Fermi level was shown to drive thickness-dependent quantum oscillations of various physical and chemical properties [22–26]. In atomic-scale 1D systems, most of the previous works studied QWSs of atom-manipulated atomic chain systems on metallic surfaces [27–29]. These works have difficulties in decoupling the electronic states at Fermi level from those of metallic substrates [27,28] and in extending the chain length [30]. Partly because of such difficulties, the length-dependent quantum oscillation has been rarely demonstrated in atomic chain systems.

In this Letter, we show that Si adatoms on Si(111)-(5 × 2)-Au atomic wires act as strong scatterers to confine and quantize 1D electrons. The wire segments with a length between 1.5 and 10.5 nm as defined by two neighboring adatoms were investigated systematically by STM/S. One-dimensional QWSs are well resolved in both filled and empty states, whose spatial distributions and energy dependence on the wire length are fully consistent with the 1D quantum box model and the band structure calculated [12]. This work clearly denies the doping role of a Si adatom as a charged impurity onto bare parts of the wires. The electron quantization is shown to give rise to a $4a_0$ [$a_0 = 0.384$ nm, the Si(111) lattice constant] quantum oscillation of the zero bias conductance. This Letter introduces a new platform for the quantitative exploitation of various quantum properties of atomic-scale 1D systems.

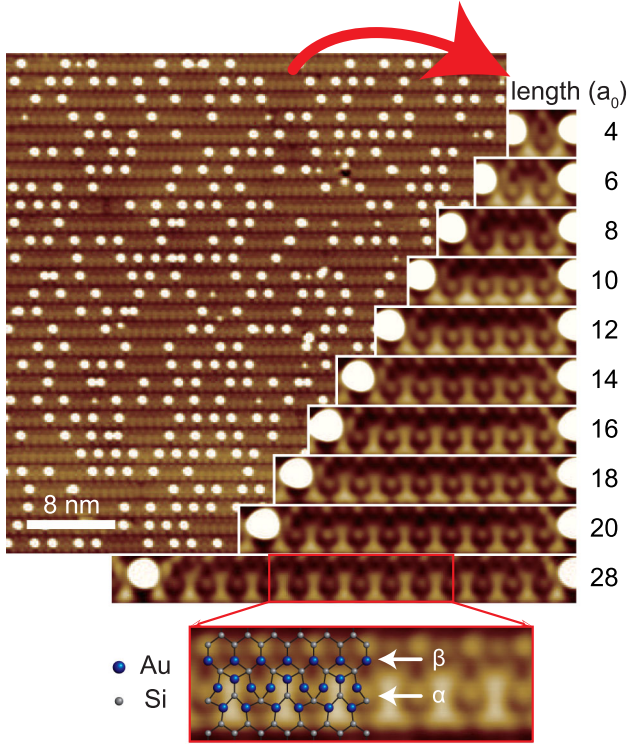


FIG. 1 (color online). Topographic STM image ($45.3 \times 45.3 \text{ nm}^2$) of Si(111)-(5 \times 2)-Au at 78.2 K and close-ups for wire segments between two Si adatoms of varying separation. The images are taken at -1.5 (large image) and -1.0 V (wire segments) sample bias. Schematics of the most recent structural model [12] are shown for the central part of the wire segment in the bottom (blue (large) and silver (small) spheres indicate Au and Si atoms, respectively).

Experiments were performed using a commercial low-temperature STM (Unisoku, Japan) at 78 K. The clean Si(111)-(7 \times 7) surface was prepared by repeated flash heating to 1520 K. Gold was evaporated onto the clean Si(111)-(7 \times 7) surface held at 932 K. At the Au coverage of 0.6–0.7 monolayer, well-ordered (5 \times 2)-Au surfaces were reproducibly formed [31,32]. For STS measurements, current-voltage (I - V) curves were recorded with the feedback loop switched off at a set point of 0.3 nA and -1.0 V.

Figure 1 shows STM images of the Si(111)-(5 \times 2)-Au surface. Well-ordered atomic wires with a 5 \times 2 unit cell are observed, which are decorated with Si adatoms appearing as bright protrusions. The atomic wires are segmented by Si adatoms, whose lengths (distance between two neighboring adatoms) are preferentially even multiples of a_0 [14]. This is due to the atomic structure of the wire with a $2a_0$ unit cell along wires [12]. The wire segment with a length of odd multiples of a_0 has an energetically unfavorable dislocation [18]. In this Letter, we focus only on the defect-free even- a_0 -length wires. As shown in Fig. 1, we can sample wire segments with varying lengths from $4a_0$ to $28a_0$ for a systematic length-dependent study. The very long segment of $28a_0$ is important to clarify the atomic structure of a

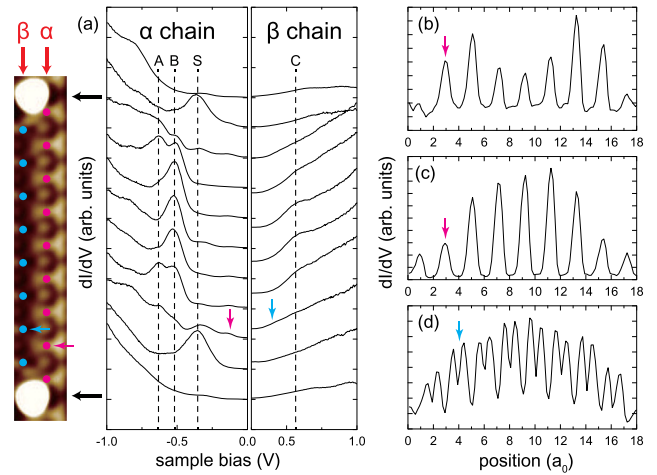


FIG. 2 (color online). (a) Spatially resolved dI/dV curves of a $18a_0$ wire. The curves are sampled for uniformly spaced positions specified in the figure (magenta and blue) from extensive (108 points) line scans of dI/dV along the α (for filled states) and the β (for empty states) chains. The whole data sets are shown in the Supplemental Material [35] (Fig. S1). The top and bottom curves are for the adatom locations (black arrows). Four prominent peaks A, B, C, and S are specified on the curves. dI/dV spatial profiles measured for the biases (b) -0.63 , (c) -0.53 , and (d) $+0.57$ V corresponding to the LDOS of A, B, and C states, respectively. These data are taken from the same dI/dV line scans as (a).

pristine wire, which is not perturbed by adatoms. A detailed topography for the central unit cells of the $28a_0$ wire is perfectly matched with the simulation based on the recently proposed structural model [12,33]. One important message is that the characteristic $\times 2$ reconstruction is maintained well away from Si adatoms. This finding contradicts with the previous structure model where the $\times 2$ structure is induced only by the doping from Si adatoms [34]. This also casts strong doubts on the observation of the local doping effect of adatoms in the previous STS result [20], which is discussed in detail below.

Electronic structures of wire segments with different lengths are investigated by the spatially resolved differential conductivity (dI/dV). We define two representative parts of a wire, α in the middle of triple $2a_0$ Au chains and β along the single $1a_0$ Au chain, which exhibit distinctive spectra (see Figs. 1 and 2). The dI/dV curves on these chains change significantly not only for different lengths but also for different locations along a wire segment. We show the dI/dV curves of a $18a_0$ wire representatively in Fig. 2. The characteristic electronic states of the α (β) chain appear noticeably in the filled (empty) state, which disappear on adatom locations (the top and bottom spectra). Four distinct spectral features, the local density of states (LDOS) maxima, are identified at -0.63 , -0.53 , $+0.57$, and -0.35 V sample biases and labeled as A, B, C, and S states, respectively. While the state A appears remarkably around 1/4 and 3/4 positions of the wire length, the B and C states are dominant at the middle of the segment.

In contrast, the S state appears only in the vicinity, about a single neighboring unit cell, of adatoms and is, thus, considered as an edge state of the segment or the state due to the doped electrons [12], which is out of the present interest. These observations clearly evidence the strong electronic perturbation by adatoms and the strong spatial dependence in the electronic structure within a wire segment. We observe the consistent trend for whole wire lengths investigated.

The spatial variations of the A , B , and C states are more systematically shown in dI/dV profiles for corresponding sample biases [Figs. 2(b)–2(d)]. These data exhibit the LDOS variations of the A , B , and C states within the wire segment. A $2a_0$ -period rapid oscillation is observed commonly for all states, which reflects the $\times 2$ periodicity of the lattice. The additional slowly varying envelopes, on the other hand, exhibit the electronic structure modulation by the extrinsic factor, that is, the edge adatoms. We observe two types of envelopes. That of state A exhibits three nodes at the ends and the middle and two antinodes at the $1/4$ and the $3/4$ positions. Those for B and C have two nodes at the end and one antinode at the middle, being qualitatively different from the former. These envelopes are the fingerprint of QWSs of the longest ($n = 1$) and the second longest ($n = 2$) electron wavelengths.

Further clarification of the QWS nature is accomplished by the extensive length dependence study. In Fig. 3(a), we show the dI/dV curves of wire segments with lengths of $10a_0$, $14a_0$, $18a_0$, and $28a_0$. One can clearly see the length-dependent energy shifts for at least A and C , which approach Fermi level as the length increases. There also exist small energy shifts for B as shown in Fig. 3(b). This length dependence can be analyzed quantitatively with the simple 1D quantum box model. If we consider that two edge adatoms of a wire segment function as confinement potentials, 1D electrons within a segment would be quantized. The n th QWS energy is given by

$$E_n = E_F + E_0 \pm \frac{h^2}{8m_e} \left(\frac{n}{L}\right)^2, \quad (1)$$

where E_F is the Fermi level, E_0 the band-edge energy, h the Planck constant, m_e the effective electron mass, and L the wire length. The plus and minus signs stand for the electronlike and holelike bands, respectively. Different band origins cause the electron wavelength, and, in turn, the QWS energy changes in opposite ways. Figures 3(b) and 3(c) compare the length-dependent energies of states A , B , and C . They unambiguously depend on inverse squares of lengths ($1/L^2$) as expected from the quantum box model. Moreover, the slope for A is approximately 4 times larger than that for B , which is also expected in the model for $n = 2$ and $n = 1$ QWSs. This is consistent with spatial envelopes of these states discussed above. The QWS energy follows the ideal $1/L^2$ law nicely despite the finite confinement

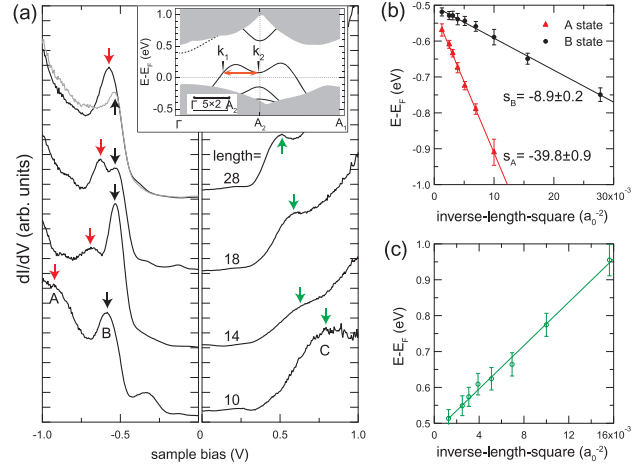


FIG. 3 (color). (a) dI/dV curves of selected wire segments (the length is given in a_0 units) with three QWSs: A (red arrows), B (black), and C (green) states. Filled state (empty state) curves are recorded from the $1/4$ (center) position of α (β) chain. Curves are vertically offset for comparison. Whole spectral features are shown in the Supplemental Material [35] (Fig. S2). The energies measured for states (b) A , B , and (c) C are plotted as a function of the inverse-length-square of wire segments. Solid lines indicate the linear fits with the slopes for A (s_A) and B (s_B) are -39.8 ± 0.9 and -8.9 ± 0.2 (arb. units), respectively. Inset: the calculated surface state band dispersions for the adatom-free Si(111)-(5 × 2)-Au surface [12]. $(k_2 - k_1)/2$ is a scattering wave vector (orange arrow) [36] near the Fermi level, which is approximately $2\pi/8a_0$. The dashed band has less weights in the topmost layer.

potentials in reality, indicating a sufficiently strong potential of adatoms for the restricted energy range of the present investigation (~ 0.5 eV). These analyses confirm solidly the 1D electron quantization within wire segments.

Based on this model, the difference in the sign of the slopes (A and B , and C) would indicate the hole and electron band nature of the corresponding bands, respectively. This is consistent with the band dispersions calculated and shown in the inset of Fig. 3(a) [12]. As expected qualitatively, the filled (empty) state bands are holelike (electronlike). For a more quantitative comparison, the electronic state (band) energies for an infinite wire are estimated from a linear extrapolation of the experimental data. The fits yield $E_0 = -0.51$ eV for the holelike band (A and B merging) and $+0.47$ eV for the electronlike band (C). This result is reasonably consistent with the band calculation, in very good agreement with the band-edge energy of especially the empty surface state. Specifically, the A and B (C) states arise predominantly from the p and d (s) atomic orbitals of Au surface atoms [37]. In filled states, there is a quantitative difference in the extrapolated and calculated energies, which comes partly from the ambiguity due to the presence of multiple surface state bands. Nevertheless, we can confidently conclude that the wire segment determined by two Si adatoms exhibits the 1D electron quantization. That is, the Au-Si metallic atomic

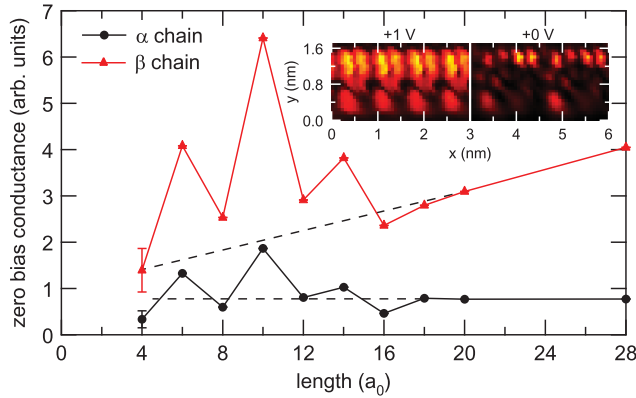


FIG. 4 (color). Length-dependent zero bias conductances measured for α and β chains. All the conductance values are extracted from the average between ± 15 mV biases, over corresponding chains to wipe out fine spatial modulations. Dotted lines display the extrapolation of the values at long chains. Inset: dI/dV maps measured for four central 5×2 unit cells of the $28a_0$ wire segment at +1 (left) and +0 V (right) biases.

wires are segmented by Si adatoms into an ensemble of quantum rods.

The electron quantization commonly causes the significant oscillatory change in various physical and chemical quantities [22–24,38]. All those quantum oscillations basically come from the DOS oscillation at Fermi level due to the matching of the quantum well width with the multiple of half the Fermi wavelength. In the present case, the wire has one metallic band whose principal Fermi wavelength ($2k_1$) is close to $4a_0$. This yields only a trivial $2a_0$ quantum oscillation since we have only wires with a length of even multiples of a_0 . However, due to the characteristic dispersion of this metallic band, an $8a_0$ Fermi scattering wavelength also emerges, corresponding to the difference between k_1 and k_2 [the orange arrow in the inset of Fig. 3(a)] [36]. Note that the exact Fermi level of the present surface could deviate from that of the calculation for an adatom-free surface. This leads to the quantum oscillation of a $4a_0$ periodicity in the DOS near the Fermi energy. Figure 4 shows the length dependence of the zero bias conductance measured on α and β chains. Both start with the lowest conductance at the shortest $4a_0$ chain and alternatively increase and decrease at $2a_0$ intervals until they reach a length of $18a_0$. In our quantization scenario, the $4a_0$ periodicity must have a direct correlation with the spatial electronic modulation at Fermi level. In the inset of Fig. 4, the dI/dV maps measured for four central unit cells of the $28a_0$ segments are shown. While the well-known $2a_0$ periodicity of the lattice is viewed at a high bias of +1 V, a clear $4a_0$ periodicity is observed near Fermi level. One can, thus, easily expect that various physical and chemical properties of individual wire segments would exhibit $4a_0$ quantum oscillations too, which can be exploited in further studies.

In contradiction with the present conclusion, the previous STM/S work interpreted the length-dependent energy shift of wire segments as the confined doping effect of adatoms [20]. This interpretation provides the length dependence of $1/L$ instead of $1/L^2$. This discrepancy is thought to come from the limited energy resolution and data sets of the previous work, which were not sufficient to distinguish the $1/L$ and $1/L^2$ dependence and to resolve the A and B QWS (see Fig. S3 of the Supplemental Material [35]). On top of the quantitative finding of the $1/L^2$ behavior, all other qualitative spectroscopic information (Figs. 2–4) support our interpretation solidly, while they are not compatible at all with the doping picture. This conclusion is fully supported by the recent structure model and the band structure calculation with and without adatoms [12]. The theoretical result indicates explicitly that the doped electrons are tightly localized near the Si adatoms; thus, the wire parts away from adatoms are not affected by these doped electrons. In fact, the well-localized electronic state induced by doping is observed (S in Fig. 2) whose energy and lateral extent are consistent with the calculation [12,37]. Meanwhile, the global doping, the change of the chemical potential defined globally, can still be possible, as established in the experimental [11] and theoretical [12] band dispersions of the present system at different Au coverages.

In summary, Si adatoms on the Si(111)-(5 × 2)-Au surface confine electrons on metallic atomic wires, resulting in the 1D electron quantization. This quantization is well supported by the energy and spatial variation of the relevant electronic states and in good consistency with the band structure calculated with a very recent structure model. The confinement also leads to a $4a_0$ -period oscillation of the LDOS at Fermi level, which is expected to bring about various quantum oscillations in the physical and chemical properties of these wire segments. With the established possibility of the Si adatom manipulation, the present result promises exciting future development of exploiting quantum rods based on self-organized atomic wires.

This work was supported by Institute for Basic Science (Grant No. IBS-R014-D1). We would like to acknowledge fruitful discussions with S. G. Kwon and M. H. Kang.

*yeom@postech.ac.kr

- [1] H. Ishii, H. Kataura, H. Shiozawa, H. Yoshioka, H. Otsubo, Y. Takayama, T. Miyahara, S. Suzuki, Y. Achiba, M. Nakatake *et al.*, *Nature (London)* **426**, 540 (2003).
- [2] O. M. Auslaender, A. Yacoby, R. de Picciotto, K. W. Baldwin, L. N. Pfeiffer, and K. W. West, *Science* **295**, 825 (2002).
- [3] H. W. Yeom, S. Takeda, E. Rotenberg, I. Matsuda, K. Horikoshi, J. Schaefer, C. M. Lee, S. D. Kevan, T. Ohta, T. Nagao, and S. Hasegawa, *Phys. Rev. Lett.* **82**, 4898 (1999).

- [4] C. Zeng, P. Kent, T.-H. Kim, A.-P. Li, and H. H. Weitering, *Nat. Mater.* **7**, 539 (2008).
- [5] P. Santhanam, S. Wind, and D. E. Prober, *Phys. Rev. Lett.* **53**, 1179 (1984).
- [6] A. Das, Y. Ronen, Y. Most, Y. Oreg, M. Heiblum, and H. Shtrikman, *Nat. Phys.* **8**, 887 (2012).
- [7] S. Nadj-Perge, I. K. Drozdov, J. Li, H. Chen, S. Jeon, J. Seo, A. H. MacDonald, B. A. Bernevig, and A. Yazdani, *Science* **346**, 602 (2014).
- [8] J. Voit, *Rep. Prog. Phys.* **58**, 977 (1995).
- [9] A. Imambekov, T. L. Schmidt, and L. I. Glazman, *Rev. Mod. Phys.* **84**, 1253 (2012).
- [10] J. Park, K. Nakatsuji, T.-H. Kim, S. K. Song, F. Komori, and H. W. Yeom, *Phys. Rev. B* **90**, 165410 (2014).
- [11] W. H. Choi, P. G. Kang, K. D. Ryang, and H. W. Yeom, *Phys. Rev. Lett.* **100**, 126801 (2008).
- [12] S. G. Kwon and M. H. Kang, *Phys. Rev. Lett.* **113**, 086101 (2014).
- [13] T. Shirasawa, W. Voegeli, T. Nojima, Y. Iwasawa, Y. Yamaguchi, and T. Takahashi, *Phys. Rev. Lett.* **113**, 165501 (2014).
- [14] A. Kirakosian, R. Bennowitz, F. J. Himpsel, and L. W. Bruch, *Phys. Rev. B* **67**, 205412 (2003).
- [15] A. Kirakosian, J. Crain, J.-L. Lin, J. McChesney, D. Petrovykh, F. Himpsel, and R. Bennowitz, *Surf. Sci.* **532–535**, 928 (2003).
- [16] R. Bennowitz, J. N. Crain, A. Kirakosian, J. Lin, J. McChesney, D. Petrovykh, and F. Himpsel, *Nanotechnology* **13**, 499 (2002).
- [17] H. S. Yoon, S. J. Park, J. E. Lee, C. N. Whang, and I.-W. Lyo, *Phys. Rev. Lett.* **92**, 096801 (2004).
- [18] P.-G. Kang, H. Jeong, and H. W. Yeom, *Phys. Rev. Lett.* **100**, 146103 (2008).
- [19] S. C. Erwin, *Phys. Rev. Lett.* **91**, 206101 (2003).
- [20] I. Barke, S. Polei, V. v. Oeynhausen, and K.-H. Meiwes-Broer, *Phys. Rev. Lett.* **109**, 066801 (2012).
- [21] M. Ono, T. Nishio, T. An, T. Eguchi, and Y. Hasegawa, *Appl. Surf. Sci.* **256**, 469 (2009).
- [22] P. J. Feibelman, *Phys. Rev. B* **27**, 1991 (1983).
- [23] Z. Zhang, Q. Niu, and C.-K. Shih, *Phys. Rev. Lett.* **80**, 5381 (1998).
- [24] T.-C. Chiang, *Surf. Sci. Rep.* **39**, 181 (2000).
- [25] M. H. Upton, C. M. Wei, M. Y. Chou, T. Miller, and T.-C. Chiang, *Phys. Rev. Lett.* **93**, 026802 (2004).
- [26] Y. Guo, Y.-F. Zhang, X.-Y. Bao, T.-Z. Han, Z. Tang, L.-X. Zhang, W.-G. Zhu, E. G. Wang, Q. Niu, Z. Q. Qiu, J.-F. Jia, Z.-X. Zhao, and Q.-K. Xue, *Science* **306**, 1915 (2004).
- [27] N. Nilius, T. M. Wallis, and W. Ho, *Science* **297**, 1853 (2002).
- [28] S. Fölsch, P. Hyltdgaard, R. Koch, and K. H. Ploog, *Phys. Rev. Lett.* **92**, 056803 (2004).
- [29] S. Fölsch, J. Yang, C. Nacci, and K. Kanisawa, *Phys. Rev. Lett.* **103**, 096104 (2009).
- [30] T. F. Mocking, P. Bampoulis, N. Oncel, B. Poelsema, and H. J. Zandvliet, *Nat. Commun.* **4**, 2387(2013).
- [31] I. Barke, F. Zheng, S. Bockenhauer, K. Sell, V. v. Oeynhausen, K. H. Meiwes-Broer, S. C. Erwin, and F. J. Himpsel, *Phys. Rev. B* **79**, 155301 (2009).
- [32] J. Kautz, M. W. Copel, M. S. Gordon, R. M. Tromp, and S. J. van der Molen, *Phys. Rev. B* **89**, 035416 (2014).
- [33] E. H. Do and H. W. Yeom (to be published).
- [34] S. C. Erwin, I. Barke, and F. J. Himpsel, *Phys. Rev. B* **80**, 155409 (2009).
- [35] See the Supplemental Material at <http://link.aps.org/supplemental/10.1103/PhysRevLett.115.266803> for technical aspects of the data analysis.
- [36] J. E. Hoffman, Ph.D. thesis, University of California, Berkeley, 2003.
- [37] S. G. Kwon and M. H. Kang (private communication).
- [38] A. Sanchez, S. Abbet, U. Heiz, W.-D. Schneider, H. Häkkinen, R. Barnett, and U. Landman, *J. Phys. Chem. A* **103**, 9573 (1999).